Journal of Molecular Structure 1075 (2014) 370–376

Contents lists available at ScienceDirect

Journal of Molecular Structure

journal homepage: www.elsevier.com/locate/molstruc

Complexes of platinum and palladium with β-diketones and DMSO: Synthesis, characterization, molecular modeling, and biological studies

J. do Couto Almeida [a], I.M. Marzano [b], F.C. Silva de Paula [b], M. Pivatto [a], N.P. Lopes [c], P.C. de Souza [d], F.R. Pavan [d], A.L.B. Formiga [e], E.C. Pereira-Maia [b], W. Guerra [a,*]

[a] Instituto de Química, Universidade Federal de Uberlândia, Campus Santa Mônica, 38.400-902 Uberlândia, MG, Brazil
[b] Departamento de Química, Universidade Federal de Minas Gerais, Campus Pampulha, 31.270-901 Belo Horizonte, MG, Brazil
[c] Núcleo de Pesquisa em Produtos Naturais e Sintéticos (NPPNS), Faculdade de Ciências Farmacêuticas de Ribeirão Preto, Universidade de São Paulo, 14.040-903 Ribeirão Preto, SP, Brazil
[d] Faculdade de Ciências Farmacêuticas, Departamento de Ciências Biológicas, Universidade Estadual Paulista, Campus Araraquara, 14.801-902 Araraquara, SP, Brazil
[e] Instituto de Química, Universidade de Campinas, 13083-970 Campinas, SP, Brazil

HIGHLIGHTS

- Four new complexes with mixed ligands were synthesized and characterized.
- Theoretical data show good agreement with the experimental results.
- The platinum complexes are more cytotoxic than the free ligands and carboplatin.
- Microbiological assays against *Mycobacterium tuberculosis* were performed.

GRAPHICAL ABSTRACT

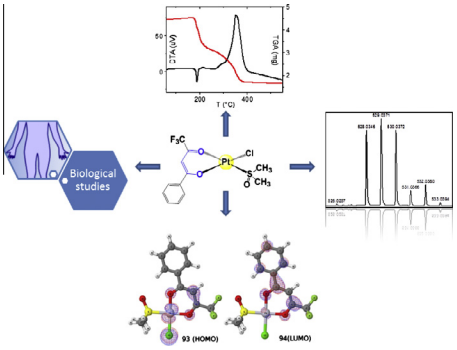

ARTICLE INFO

Article history:
Received 14 April 2014
Received in revised form 18 June 2014
Accepted 9 July 2014
Available online 18 July 2014

Keywords:
Metal complexes
Molecular modeling
β-Diketones
Mycobacterium tuberculosis
Cytotoxic activity

ABSTRACT

This work reports on the synthesis and characterization of new complexes of the type [MCl(L)DMSO], where L = 4,4,4-trifluoro-1-phenyl-1,3-butanedione (HTPB) or 4,4,4-trifluoro-1-(2-thienyl)-1,3-butanedione (HTTA) and M = Pt^{2+} or Pd^{2+}. These complexes were characterized by elemental analyses, conductivity measurements, FT-IR, UV–Vis, high-resolution mass spectra (HRESIMS) and TG/DTA. In the complexes, the metallic ions bind to β-diketone *via* the oxygen atoms and to DMSO molecule *via* sulfur atom. The structures of complexes were optimized and theoretical data showed good agreement with the experimental results. The cytotoxic activity of the compounds was evaluated in a chronic myelogenous leukemia cell line. The platinum complexes were more cytotoxic than the free ligands and carboplatin and are promising candidates for further investigations. As example, the compound [PtCl(TPB)(DMSO)] inhibits the growth of K562 cells with an IC_{50} value equal to 2.5 μM. Furthermore, microbiological assays against *Mycobacterium tuberculosis* showed that all complexes exhibit low cytotoxicity against this bacterial strain while the free ligands exhibited MIC values of approximately 10 μg mL^{-1}.

* Corresponding author. Address: Instituto de Química, Universidade Federal de Uberlândia, Av. João Naves de Ávila, 2121, Campus Santa Mônica, 38.400-902 Uberlândia, MG, Brazil. Tel.: +55 34 3239 4143; fax: +55 34 3239 4208.
E-mail address: wg@iqufu.ufu.br (W. Guerra).

http://dx.doi.org/10.1016/j.molstruc.2014.07.023
0022-2860/

Introduction

Cisplatin, one of the most important chemotherapeutic agents for the treatment of a wide spectrum of solid tumors, has several side effects. These undesirable effects led to the development of a second generation of drugs, such as carboplatin and oxaliplatin [1,2]. However, carboplatin has a spectrum of action similar to that observed for cisplatin and, the oxaliplatin exhibits a specificity to treat colon cancer. Moreover, for all platinum complexes used in cancer chemotherapy, an intrinsic or acquired resistance leads to a failure in the treatment [3]. Thus, in an attempt to reduce toxicity, the resistance and wide spectrum of activity, thousands of platinum complexes have been prepared by varying the nature of the leaving groups and the carrier ligands [4,5]. Indeed, much attention has been focused on designing new platinum complexes with improved pharmacological properties and a broader range of antitumor activity [6]. It should be noted that the development of new non-platinum compounds with antitumoral activity also is a field in full development with results very interesting. In this aspect, several palladium complexes have been obtained aiming to produce new drugs. These compounds have potential as anticancer and anti-infective agents [7–9].

On the other hand, the properties of β-diketones are of great interest because these compounds are useful as metal extracting agents [10,11] and most recently as potential drugs [12–14]. For example, Wilson et al. showed that platinum complexes containing β-diketones exhibit anticancer activity against several tumoral cells strains [13]. Our research group also showed that a copper(II) complex with 4,4,4-trifluoro-1-(2-thienyl)-1,3-butanedione and 2,2-bipyridine inhibits the growth of K562 cells with an IC_{50} value equal to 28.2 μmol L^{-1} [15]. These findings can lead to a more rational design of new complexes in order to establish a structure–activity relationship. Thus, these observations encourage us to synthesize a new series of complexes containing β-diketones as possible antitumoral and antibacterial agents. Therefore, this paper reports on the synthesis of new complexes of Pt(II) and Pd(II) containing 4,4,4-trifluoro-1-(2-thienyl)-1,3-butanedione (HTTA) and 4,4,4-trifluoro-1-phenyl-1,3-butanedione (HTPB), their characterization and antimicrobial and cytotoxic activities.

Experimental

Physical measurements

Conductivity studies were carried out with a Digimed DM 31 conductivity meter using a cell of constant 1.00 cm^{-1}, spectroscopic grade dimethyl sulfoxide (Merck) (Λ_M = 0.96 μs/cm) and tetraethylammonium bromide (Λ_M = 79.19 μs/cm) were used as a standard compounds.

Elemental analyses were performed using a Perkin-Elmer 2400 CHNS Elemental Analyser. Analyses by atomic absorption (% metal) were made in a spectrophotometer Hitachi 8200.

IR spectra were registered in KBr pellets on a Shimadzu FTIR-Irprestige-21 spectrometer.

Spectrophotometer UV-2501 PC Shimadzu was used for UV and visible absorption measurements.

High-resolution mass spectra (HRESIMS) with electrospray ionization were measured on an ultrOTOF (Bruker Daltonics) spectrometer, operating in the positive mode. Acetonitrile was used as solvent system and the samples were infused into the ESI source at a flow rate of 5 μL/min. The calculated values for the charged complex ions were made using ChemDraw Ultra 12.0.

Thermogravimetric analyses (TG/DTA) were obtained on a TGA-50 Shimadzu, using 6.0 mg samples packed in aluminum crucible. Samples were heated at 10 °C/min from room temperature to 600 °C, in a dynamic nitrogen atmosphere (flow rate of 200 mL/min).

Starting materials

The compound *cis*-$[PtCl_2(DMSO)_2]$ was prepared according to the literature [16]. The reagents (ligands and metal salts) are commercially available (Aldrich). All other chemicals reagents were of analytical grade, purchased from different sources, and used without prior purification.

Preparation of the complexes

The complexes were synthesized following the procedures described below:

a) $[Pd(TTA)_2]$

This complex was first synthesized by Okeya et al. using a different method [17]. In this work, 0.163 g of K_2PdCl_4 (0.5 mmol) previously dissolved in water was added to 5 mL of an ethanolic solution of 4,4,4-trifluoro-1-(2-thienyl)-1,3-butanedione (1.0 mmol). The mixture was stirred for 48 h and the solid formed was separated by filtration, washed with water, ethanol and dried under reduced pressure.

Yield: 81%. Color: Yellow. Anal. Calcd. for $[Pd(C_8H_4F_3O_2S)_2]$: C, 35.02; H, 1.47; S, 11.69; Pd, 19.39%; Found: C, 34.80; H, 1.36; S, 11.39; Pd 18.91%. IR spectra in KBr, ν (cm^{-1}): 3100, 3095, 3079, 1578, 1536, 1507, 1434, 1405, 1354, 1317, 1261, 1234, 1185, 1151, 1068, 942, 861, 795, 727, 713, 609, 565, 523, 493, 476, 458, 423. UV–Vis (ethanol): λ_{max} (nm) = 283 (9.36×10^3 mol^{-1} L cm^{-1}), 330 (1.86×10^4 mol^{-1} L cm^{-1}), 364 (2.27×10^4 mol^{-1} L cm^{-1}). ΛM = 2.20 μs/cm.

b) [PtCl(TTA)(DMSO)]

0.25 mmol of *cis*-$[PtCl_2(DMSO)_2]$ previously dissolved in warm water (5 mL, 60–70 °C) was added to 5 mL of an aqueous solution of 4,4,4-trifluoro-1-(2-thienyl)-1,3-butanedione (1.0 mmol). The mixture was stirred for 48 h and the solid formed was separated by filtration, washed with water, ethanol and dried under reduced pressure.

Yield: 71%. Color: Yellow. Anal. Calcd. for $[Pt(C_8H_4F_3O_2S)(C_2H_6SO)Cl]$: C, 22.67; H, 1.90; S, 12.10; Pt, 36.82%; Found: C, 22.95; H, 1.91; S, 12.06; Pt, 36.94%. IR spectra in KBr, ν (cm^{-1}): 3083, 3016, 2922, 1573, 1537, 1411, 1349, 1312, 1270, 1260, 1197, 1133, 1029, 939, 793, 745, 691, 608, 561, 532, 446. UV–Vis (ethanol): λ_{max} (nm) = 295 (4.58×10^3 mol^{-1} L cm^{-1}), 361 (1.41×10^4 mol^{-1} L cm^{-1}). ΛM = 1.98 μs/cm.

c) [PdCl(TTA)(DMSO)]

To a solution containing 0.163 g of K_2PdCl_4 (0.5 mmol) previously dissolved in water, was added 0.5 mmol of DMSO. After 1 h of stirring, 0.5 mmol of 4,4,4-trifluoro-1-(2-thienyl)-1,3-butanedione previously dissolved in ethanol was added. The mixture was stirred for 24 h and the solid formed was separated by filtration, washed with water, methanol and dried under reduced pressure.

Yield: 48%. Color: Yellow. Anal. Calcd. for $[Pd(C_8H_4F_3O_2S)(C_2H_6SO)Cl]$: C, 27.22; H, 2.28; S, 14.54; Pd, 24.12 Found: C, 27.22; H, 1.80; S, 14.01; Pd, 24.44. IR spectra in KBr, ν (cm^{-1}): 3083, 3023, 2365, 1571, 1404, 1306, 1208, 1132, 1018, 936, 860, 785, 747, 671, 603. UV–Vis (ethanol): λ_{max} (nm) = 283 (1.06×10^4 mol^{-1} L cm^{-1}), 332 (1.77×10^4 mol^{-1} L cm^{-1}), 361 (2.13×10^4 mol^{-1} L cm^{-1}). ΛM = 2.73 μs/cm.

d) [Pd(TPB)$_2$]

This complex was also first synthesized by Okeya et al. using a different method [17]. In this work, 0.082 g of K_2PdCl_4 (0.25 mmol) previously dissolved in water was added to 5 mL of an methanolic solution of 4,4,4-trifluoro-1-phenyl-1,3-butanedione (0.50 mmol) with triethylamine to a pH 6.3. The mixture was stirred for 24 h and the solid formed was separated by filtration, washed with water, methanol and dried under reduced pressure.

Yield: 61%. Color: Yellow. Anal. Calcd. for [Pd($C_{10}H_6F_3O_2$)$_2$]: C, 44.76; H, 2.24; Pd, 19.83. Found: C, 45.08; H, 1.53; Pd, 19.81. IR spectra in KBr, ν (cm^{-1}): 2370, 2345, 1593, 1568, 1540, 1529, 1509, 1490, 1451, 1437, 1420, 1324, 1312, 1297, 1255, 1193,1181, 1163, 1147, 1097, 1075, 1027, 1000, 975, 949, 930, 843, 816, 804, 766, 730, 708, 691, 612, 565, 525, 458, 420. UV–Vis (ethanol): λ_{max} (nm) = 272 (1.88×10^4 mol^{-1} L cm^{-1}), 300 (2.17×10^4 mol^{-1} L cm^{-1}), 359 (1.12×10^4 mol^{-1} L cm^{-1}). ΛM = 1.20 μs/cm.

e) [PtCl(TPB)(DMSO)]

To *cis*-[PtCl$_2$(DMSO)$_2$] (0.25 mmol) in warm water (5 mL, 60–70 °C), 4,4,4-trifluoro-1-phenyl-1,3-butanedione (0.25 mmol) dissolved in methanol (5 mL) was added. After stirring for 48 h at room temperature the solid formed was separated by filtration, washed with water, methanol and dried under reduced pressure.

Yield: 40%. Color: Yellow. Anal. Calcd. for [Pt($C_{10}H_6F_3O_2$)(C_2H_6SO)Cl]: C, 27.51; H, 2.31; S, 6.12; Pt, 37.25. Found: C, 28.08; H, 2.01; S, 6.25, Pt, 36.83. IR spectra in KBr, ν (cm^{-1}): 3029, 3010, 2931, 1599, 1566, 1539, 1486, 1460, 1394, 1322, 1302, 1256, 1190, 1144, 1032, 939, 808, 774, 735, 689, 603, 557, 452. UV–Vis (ethanol): λ_{max} (nm) = 271 (8.04×10^3 mol^{-1} L cm^{-1}), 319 (1.57×10^4 mol^{-1} L cm^{-1}). ΛM = 2.29 μs/cm.

f) [PdCl(TPB)(DMSO)]

This complex was synthesized using the same method described for the compound [PdCl(TTA)(DMSO)].

Yield: 19%. Color: Yellow. Anal. Calcd. for [Pd($C_{10}H_6F_3O_2$)(C_2H_6SO)Cl]: C, 33.12; H, 2.78; S, 7.37; Pd, 24.46. Found: C, 33.08; H, 2.94; S, 7.01; Pd, 23.96. IR spectra in KBr, ν (cm^{-1}): 3031, 2924, 2365, 1593, 1571, 1541, 1488, 1457, 1420, 1321, 1291, 1268, 1185, 1132, 1079, 1034, 951, 807, 761, 717, 679, 596, 557. UV–Vis (ethanol): λ_{max} (nm) = 274 (5.47×10^4 mol^{-1} - L cm^{-1}), 354 (2.61×10^4 mol^{-1} L cm^{-1}). ΛM = 1.68 μs/cm.

Molecular modeling

Geometry optimizations were carried out using GAMESS software [18] with a convergence criterion of 10^{-4} a.u. in a conjugated gradient algorithm without constraints. The LANL2DZ effective core potential [19] was used for platinum and palladium and the atomic 6-31G(d) basis set [20] for all other atoms. Density functional theory (DFT) calculations were carried out using PBE0 [21] gradient-corrected hybrid to solve the Kohn–Sham equations with a 10^{-5} a.u. convergence criterion for the density change.

Vibrational frequency analyses were performed at the same level of theory to confirm the structures as minima of the potential energy surfaces (PES) showing no imaginary frequencies.

Zero-point energies from these calculations were used to correct total energies and compare the stability of isomers. The harmonic frequencies (without scaling) and intensities were used to generate the theoretical spectra. The corresponding simulated vibrational spectra were obtained from the sum of Lorentzian functions with 20 cm^{-1} half-bandwidths as reported before [22].

Time Dependent-DFT was used to obtain electronic spectra of all structures under the same level of theory with the calculation of the 30 lowest singlet states. Simulated UV–Vis spectra were obtained from the sum of Gaussian functions with 2000 cm^{-1} half-bandwidths. All the models and figures were plotted using Jmol [23].

Cells and culture

The K562 cell line was purchased from the Rio de Janeiro Cell Bank (number CR083 of the RJCB collection). This cell line was established from pleural effusion of a 53 year-old female with chronic myelogenous leukemia in terminal blast crisis. Cells were cultured in RPMI 1640 (Sigma Chemical Co.) medium supplemented with 10% fetal calf serum (CULTILAB, São Paulo, Brazil) at 37 °C in a humidified 5% CO_2 atmosphere. Cultures grow exponentially from 10^5 cells mL^{-1} to about 8×10^5 cells mL^{-1} in three days. Cell viability was checked by Trypan Blue exclusion. The cell number was determined by coulter counter analysis.

For cytotoxicity assessment, 1×10^5 cells mL^{-1} was cultured for 72 h in the absence and presence of a range of concentrations of tested compounds. The sensitivity to compound was evaluated by the concentration that inhibits cell growth by 50%, IC_{50}. Stock solutions were prepared in DMSO.

Anti-Mycobacterium tuberculosis activity assay

The anti-MTB activity of the compounds was determined by the REMA (Resazurin Microtiter Assay) method according to Palomino et al., [24]. Stock solutions of the tested compounds were prepared in dimethyl sulfoxide (DMSO) and diluted in Middlebrook 7H9 broth (Difco) supplemented with oleic acid, albumin, dextrose and catalase (OADC enrichment – BBL/Becton–Dickinson), to obtain final drug concentration ranges of 0.09–25 μg/mL. A serial dilution was performed on the equipment Precision™ XS (Biotek). The rifampicin was dissolved in distilled water, and used as a standard drug. A suspension of the MTB H37Rv ATCC 27294 was cultured in Middlebrook 7H9 broth supplemented with OADC and 0.05% Tween 80. The culture was frozen at −80 °C in aliquots. After two days was carried out the CFU/mL of an aliquot. The concentration was adjusted by 5×10^5 UFC/mL and 100 μL of the inoculum was added to each well of a 96-well microtiter plate together 100 μL the compounds. Samples were set up in triplicate. The plate was incubated for 7 days at 37 °C. After 24 h 30 μL of 0.01% resazurin (solubilized in water) was added. The fluorescence of the wells was read after 24 h by TECAN Spectrafluor®. The MIC was defined as the lowest concentration resulting in 90% inhibition of growth of MTB.

Results and discussion

Four new complexes containing 4,4,4-trifluoro-1-(2-thienyl) -1,3-butanedione (HTTA) or 4,4,4-trifluoro-1-phenyl-1,3-butanedione (HTPB) and dimethylsulfoxide (DMSO) as ligands were synthesized and characterized by elemental analyses, conductivity measurements, FT-IR, UV–Vis, HRMS and TG/DTA. All of the complexes are stable to air and light and soluble in organic solvents such as DMSO and DMF. The chemical structures of the ligands HTTA, HTPB and complexes containing HTTA are presented in Fig. 1.

The results of the elemental analyses (C, H, S and metal) are in accordance with the proposed structures.

The molar conductivity values of solutions (10^{-3} M; DMSO or acetonitrile) for all complexes were far below that of the 1:1 standard electrolyte indicating that they are not charged [25].

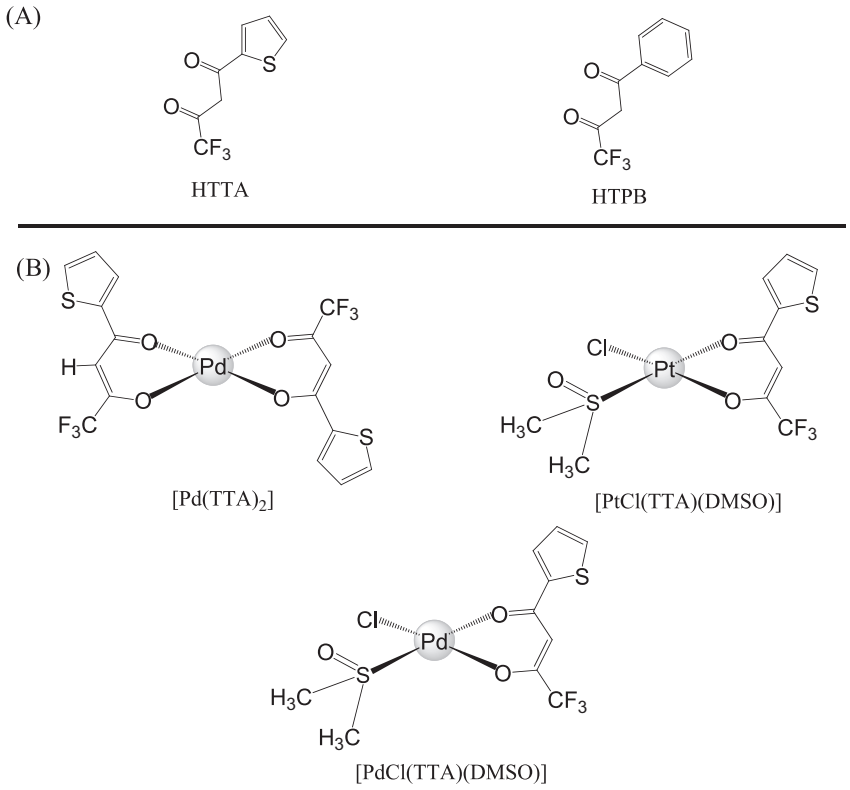

Fig. 1. (A) Ligands (HTTA and HTPB). (B) Complexes with HTTA.

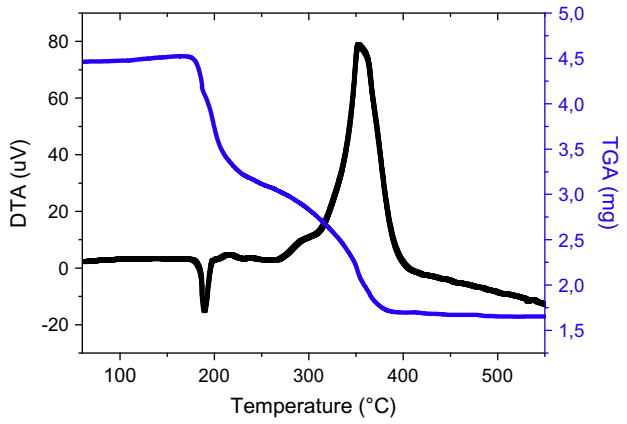

Fig. 2. TGA/DTA curve of complex [PtCl(TTA)(DMSO)].

The same pattern was found when the complexes were dissolved in DMSO, even after 30 min.

Thermal analyses

The thermal analyses for all compounds with HTTA and HTPB were carried out between room temperature and 600 °C in air atmosphere. The events observed in the TG curves of the complexes containing DMSO are very similar and only the TG curve of the platinum complex will be discussed.

The TG/DTA curve for complex [PtCl(TTA)(DMSO)] (Fig. 2) shows three events (exothermic and endothermic) of weight loss at 130–480 °C range due to the complex thermal decomposition (loss of the ligands) corresponding to 63.19.% (calcd: 63.18%). At 600 °C there is a residue (elemental platinum) corresponding to 36.99% (calcd: 36.82%). The percentage of metal fits well with the proposed formulas for all complexes with DMSO. % Pd calcd. for complex [PdCl(TPB)(DMSO)] is 24.46 (found: 24.80). Curiously, for the complex [PdCl(TTA)(DMSO)], between 390 and 590 °C occurs the oxidation of the remaining Pd^0 to Pd^{II}. Thus, at 600 °C there is a residue (palladium oxide) corresponding to 27.21% (calcd: 27.75%).

The TG and DTA curves for the decomposition of compound $[Pd(TTA)_2]$ shows two events (exothermic and endothermic) of weight loss between 120 and 450 °C, which can be attributed to the loss of the ligands, corresponding to 80.67% (calcd: 81.25%). At 500 °C there is a residue (elemental palladium) corresponding to 19.32% (calcd: 18.52%). For the complex $[Pd(TPB)_2]$, at 500 °C there is a residue (palladium) corresponding to 19.83% (calcd: 19.83%).

The inexistence of weight loss in the TG curve up to 150 °C indicates the absence of water molecule in the compounds.

IR spectra

The IR spectra of the free ligands were performed for comparison to the corresponding complexes isolated. Characteristic absorptions in the 3158–2984 cm^{-1} region were observed, corresponding to ν_{CH} and ν_{CH} (thiophene ring). Vibrational frequencies between 1660 and 1620 cm^{-1} are due to C=O group.

In the IR spectra of the complexes, the peaks due to $\nu_{C=O}$ were shifted to lower wavelengths indicating the complexation through oxygen atoms [16]. The C—H stretching of the free respective ligand is shifted toward higher frequency, as a result of metal coordination to the carbonyl oxygen atoms. For the complexes containing DMSO, the coordination was verified by the S—O stretching band near 1124 cm^{-1}, suggesting that this ligand is bound to the platinum or palladium through the sulfur atom [26]. For the complexes with HTTA, the symmetric and asymmetric CF_3 stretching

frequencies are observed at 1138 and 1314 cm^{-1}, respectively. These absorption bands appear in the infrared spectrum of the free ligand at 1120 and 1278 cm^{-1}. The absorption around 1072 cm^{-1} in the IR spectra of the complexes with HTTA should be assigned to ν(C—S). Some of the weak bands in the range of 500–463 cm^{-1} in the spectra of the complexes could tentatively be ascribed to M—O stretchings [26].

UV–Vis spectra

In order to confirm the coordination, we have analysed the spectra in the UV–visible regions in ethanol.

The UV–visible absorption spectrum of the ligand HTTA in ethanol (5×10^{-5} M) displays three bands centered at 263, 288 and 338 nm. According to Chen et al. [27], the bands centered at 338 and 263 nm can be assigned to $\pi \rightarrow \pi^*$ transitions involving the whole conjugation and delocalization electronic system of the ligand and the transition of the thiophene ring moiety. The band centered at 288 nm may be attributed to $n \rightarrow \pi^*$ transition of the keto carbonyl and enol carbonyl group of the tautomer. In Fig. 3, the spectra of ethanolic solutions of the ligand HTTA and their respective metal complexes are shown. A bathochromic shift in relation to free ligand confirms the presence of the complexes in solution. One can also notice that the band localized at 288 nm in the free ligand disappears or is observed as a shoulder of low intensity in all compounds. This result confirms the complexation and suggests that the oxygen of the β-diketone group is involved in the coordination sphere. On the other hand, the absorption spectrum of the ligand HTPB in ethanol (5×10^{-5} M) displays two bands centered at 249 and 327 nm. In the spectra of complexes, the band localized at 249 nm present a red shift (±22 nm) when compared to the organic compound free, which confirms the presence of complexes in solution.

Mass spectrometry

Mass spectra of platinum compounds (see Fig. 4) containing chlorine are typical by an isotopic cluster pattern demonstrating the presence of isotopes ^{194}Pt (32.97%), ^{195}Pt (33.83%), ^{196}Pt (25.24%), ^{198}Pt (7.16%), ^{35}Cl (75.77%) and ^{37}Cl (24.23%), with the nuclide abundance in parentheses (A%) [28]. The high-resolution mass spectra of the synthesized complexes were recorded and the obtained data confirm the proposed structures. In this work, the *m/z* values listed below in the text refer to the peak of the isotopic cluster corresponding to the ^{195}Pt and ^{35}Cl isotopes.

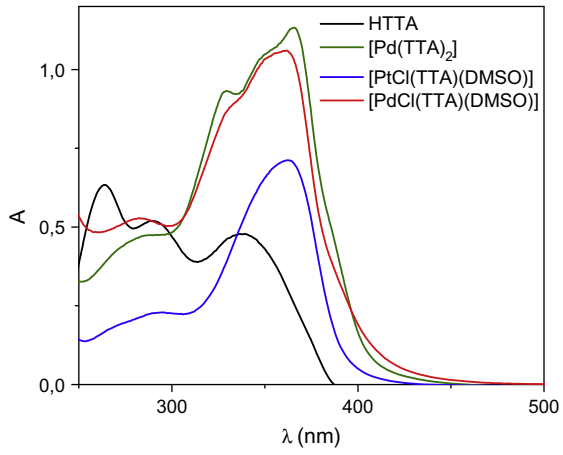

Fig. 3. Electronic spectra in ethanol (1.0×10^{-5} M).

For the complexes [PtCl(TTA)(DMSO)] and [PtCl(TPB)(DMSO)], the results indicate that these compounds suffer solvolysis, i.e., there is a replacement of chloride ion by a molecule of the solvent (acetonitrile), thus the isotopic pattern in mass spectrum also change [28]. As example (see Fig. 4), the charged complex ion peak with *m/z* 529.0371 $[M - Cl^- + CH_3CN]^+$ (calcd for [Pt(TPB)(DMSO)(CH_3CN)], 529.0372).

The mass spectrum of complex $[Pd(TPB)_2]$ exhibited the cationized ion at *m/z* 558.9583 $[M + Na]^+$ (calcd for $Pd(TPB)_2Na$, 558.9572). The same pattern was found for the complex $[Pd(TTA)_2]$ exhibiting a sodiated ion at *m/z* 570.8715 $[M + Na]^+$ (calcd for $Pd(TTA)_2Na$, 570.8701).

Molecular modeling

The obtained heteroleptic Pd(II) and Pt(II) complexes have two possible isomers with DMSO bonded *cis* or *trans* to the thiophenyl or phenyl groups of the β-diketones. In order to evaluate their relative stabilities, we have performed a theoretical investigation of all possible structures. As expected, all structures show a square-planar coordination of the d^8 M(II) ions and the bond distances are in good agreement with similar complexes. For example, M—O_{TTA} bonds range from 2.01 to 2.03 Å and M—Cl bonds are 2.31–2.32 Å. In all structures, thiophenyl and phenyl groups were found to be planar and almost co-planar with the β-diketone group. All the optimized structures, bond distances and angles can be found as Supporting Information (Figs. S1 and S2). In the cases of [PdCl(TTA)(DMSO)] and [PtCl(TTA)(DMSO)], the *trans* isomers were found to be more stable by 1.3 and 0.9 kcal mol^{-1}, respectively. For [PdCl(TPB)(DMSO)] and [PtCl(TPB)(DMSO)], the situation is reversed and the *cis* isomer is more stable by 1.6 and 2.1 kcal mol^{-1}, respectively. Even if these energies are higher than kT at 298 K (0.59 kcal mol^{-1}), the differences are very small resulting in non-zero Boltzmann distributions and co-existance of both isomers cannot be ruled out using these data.

Simulated vibrational spectra can be seen in Fig. S3 of the Supporting Information. The spectra are very similar and cannot be used to differentiate *cis* and *trans* isomers in the 400–4000 cm^{-1} range. All the spectra show the expected vibrational modes and, as an example, for complex *cis*-[PtCl(TTA)(DMSO)] the C=O and C=C stretching modes of the diketone are predicted at 1662 and 1617 cm^{-1}, respectively. The in-plane angular deformation of the C=O is found at 1384 cm^{-1} and the in-plane angular deformation of C—H from thiophenyl is predicted at 1270 cm^{-1}. The stretching mode of the C—H of the diketone is seen at 1200 cm^{-1}. These assignments are the same for all isomers and corroborate with the experimental spectra.

Using TD-DFT, the electronic spectra of all structures were predicted and can be seen in Fig. 5. Oscillator strengths and excitation energies for all calculated states can be found as Supporting Information (Tables S1 and S2). For all complexes, the simulated spectrum of the most stable isomer is very similar with the experimental profile. For Pt(II) complexes, the calculations predict two intense bands at 220 nm and 300 nm that can be compared to bands at 295 and 361 nm observed experimentally for [PtCl(TTA)(DMSO)] and 271 and 319 nm for [PtCl(TPB)(DMSO)]. Based on the orbital analysis (Supporting Information), the most intense band of the experimental spectra (~300 nm) can be ascribed to a $\pi \rightarrow \pi^*$ transition from the β-diketone ligand for both complexes with an important contribution from the thiophenyl and phenyl rings. In all cases, there is a relevant contribution of the M(II) in the ground state, suggesting a mixing of MLCT states for these bands. The observed difference between predicted and experimental transition energies was expected for TD-DFT and it has been observed before for other complexes [29].

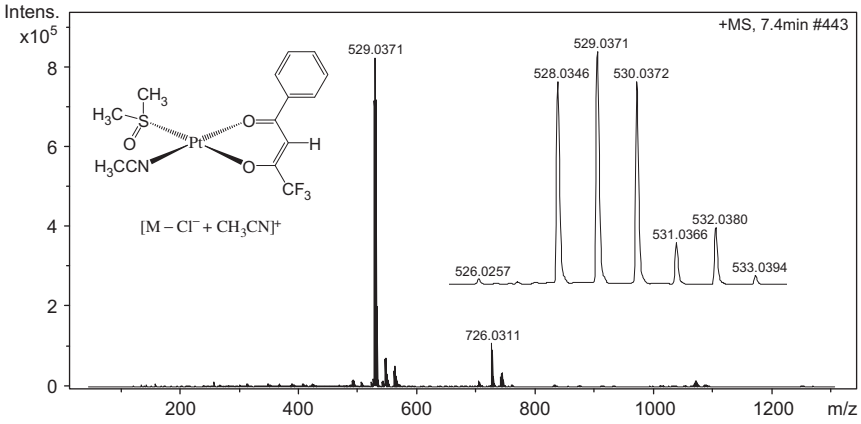

Fig. 4. HRESIMS spectrum of complex [PtCl(TPB)(DMSO)] (chloride ion was exchanged for a molecule of solvent (acetonitrile) and the charged complex ion observed was $[M - Cl^- + CH_3CN]^+$).

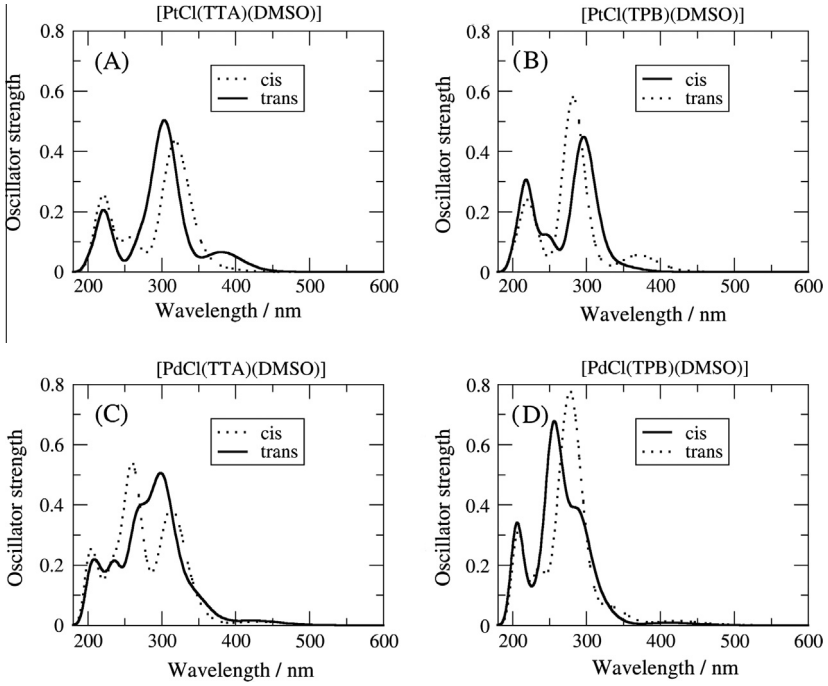

Fig. 5. TD-DFT simulated UV–Vis spectra using PBE0/LANL2DZ/6-31G(d) for (A) [PtCl(TTA)(DMSO)], (B) [PtCl(TPB)(DMSO)], (C) [PdCl(TTA)(DMSO)], and (D) [PdCl(TPB)(DMSO)]. Solid lines represent the spectra of the most stable isomers.

The theoretical spectra of Pd(II) complexes are very similar to the platinum analogs as is also seen in experiment. The only difference is the presence of a shoulder in the experimental spectra. Calculations also predict this feature and revealed that it is due to a splitting of the same transitions already observed for the Pt(II) complexes. Orbital plots, transitions and Kohn–Sham orbital compositions can be found as Supporting Information.

Cytotoxic studies

The cytotoxic efficacy of the ligands HTTA, HTPB and their complexes was examined on K562 cells. All compounds inhibit the growth of K562 cells with IC_{50} values between 2.5 and 51.92 μM (Table 1). IC50 values obtained for two platinum complexes used in chemotherapy, cisplatin and carboplatin, are also shown for the sake of comparison. As expected, the platinum complexes tested were found to be more potent than the palladium analogs and these findings were consistent with other studies conducted on platinum and palladium complexes [30–33]. For the complexes with HTTA, $[Pd(TTA)_2]$ was as active as the free ligand, whereas the activity of [PtCl(TTA)(DMSO)] was 7-fold higher when compared to

Table 1
IC_{50} values for HTTA, HTPB, cisplatin, carboplatin and complexes.

Compound	[a]IC_{50} (μM)
HTTA	51.46 ± 2.1
HTPB	7.6 ± 0.7
$[Pd(TTA)_2]$	51.92 ± 3.7
[PdCl(TTA)(DMSO)]	14.3 ± 1.2
$[Pd(TPB)_2]$	12.2 ± 1.2
[PdCl(TPB)(DMSO)]	23.0 ± 2.3
[PtCl(TTA)(DMSO)]	7.7 ± 0.8
[PtCl(TPB)(DMSO)]	2.5 ± 0.3
Carboplatin	10.0 ± 1.2
Cisplatin	1.1 ± 0.1

[a] IC_{50} is the concentration required to inhibit 50% of K562 cell growth.

Table 2
Anti-*M. tuberculosis* activity (MIC) for the ligands HTTA, HTPB and complexes.

Compound	MIC (μg/mL)
HTTA	10.89
HTPB	9.61
[Pd(TTA)$_2$]	>25.00
[PdCl(TTA)(DMSO)]	24.32
[Pd(TPB)$_2$]	>25.00
[PdCl(TPB)(DMSO)]	>25.00
[PtCl(TTA)(DMSO)]	>25.00
[PtCl(TPB)(DMSO)]	24.64

the free ligand. On the other hand, the palladium complexes with HTPB were less active when compared to free ligand, whereas the activity of [PtCl(TPB)(DMSO)] is 3-fold higher. It is worth noting that the novel complexes were less active than cisplatin in K562 cell line, but the platinum compounds were more active than carboplatin.

Lastly, the platinum complexes are more active than the ligands. This can be attributed to a higher ability of the complexes to diffuse into the cell membrane and reach their biological target. Several biological studies were performed for platinum complexes of type [PtCl(O,O′-acac)(DMSO)] and was showed that the cytotoxicity mechanisms of these complexes may not necessarily require interaction with DNA [34]. Thus, mechanistic studies and cytotoxicity of these complexes in other cell lines will be investigated in the future.

Anti-M. tuberculosis activity

The organic ligands presented anti-*M. tuberculosis* activity with MIC values less than 11 μg/mL. The minimum inhibitory concentration (MIC) values for the complexes were higher than 24 μg/mL (see Table 2), which means that they are not very active [35].

Concluding remarks

Four new complexes of Pt(II) or Pd(II) containing 4,4,4-trifluoro-1-(2-thienyl)-1,3-butanedione and 4,4,4-trifluoro-1-phenyl-1,3-butanedione were synthesized and characterized using thermal, spectroscopic and spectrometric techniques. The spectroscopic techniques showed that the ligands are coordinated to platinum or palladium by the β-diketone group. Theoretical data show good agreement with the experimental results.

The cytotoxic efficacy of the ligands and their complexes were examined on K562 cells. The platinum complexes were more effective than free ligands, displaying promising anticancer activity against K562 cells. On the contrary, the microbiological assays against *M. tuberculosis* showed that all the tested complexes exhibited low cytotoxicity, while the organic ligands presented significant activity as anti-*M. tuberculosis* and are promising candidates for further studies.

Acknowledgements

This work was supported by grants of CNPq (Conselho Nacional de Desenvolvimento Científico e Tecnológico, Brazil), RMQ (Rede Mineira de Química), Universidade Federal de Uberlândia (UFU), FAPEMIG (Fundação de Amparo à Pesquisa de Minas Gerais, Brazil) and INCT-Catálise. ALBF would like to acknowledge CENAPAD for computational time and FAPESP for financial support.

Appendix A. Supplementary material

Supplementary data associated with this article can be found, in the online version, at http://dx.doi.org/10.1016/j.molstruc.2014.07.023.

References

[1] C.X. Zhang, S.J. Lippard, Curr. Opin. Chem. Biol. 7 (2003) 481;
E.T. Cesar, R.N. Berg, A.P.S. Fontes, H. Silva, M.F. Saraiva, W. Guerra, M.V. de Almeida, Bull. Korean Chem. Soc. 28 (2007) 295.
[2] P.P. Silva, I.M. Marzano, I.P.S. Medeiros, E. Pereira-Maia, Global J. Inorg. Chem. 21 (2011) 252.
[3] I. Buß, D. Garmann, M. Galanski, G. Weber, G.V. Kalayda, B.K. Keppler, U. Jaehde, *J. Inorg. Biochem.* 105 (2011) 709;
E.C. Pereira-Maia, A. Garnier-Suillerot, J. Biol. Inorg. Chem. 8 (2003) 626.
[4] M.J. Clarke, Coord. Chem. Rev. 232 (2002) 69.
[5] W. Guerra, H. Silva, M.V. de Almeida, A.P.S. Fontes, Quím. Nova 30 (2007) 56;
W. Guerra, M.V. de Almeida, H. Silva, A.P.S. Fontes, Quím. Nova 28 (2005) 809.
[6] S.P. Fricker, Dalton Trans. 4903 (2007) 4903;
P.P. Silva, F.C.S. de Paula, W. Guerra, J.N. Silveira, F.V. Botelho, L.Q. Vieira, T. Bortolotto, F.L. Fischer, G. Bussi, H. Terenzi, E.C. Pereira-Maia, J. Braz. Chem. Soc. 21 (2010) 1237;
K.S. Lovejoy, S.J. Lippard, P. Sadler, Dalton Trans. 48 (2009) 10651–10659;
N. Farrel, Y. Qu, M.P. Hacker, J. Med. Chem. 33 (1990) 2179;
W. Guerra, I.R. Silva, E.A. Azevedo, A.R.de S. Monteiro, M. Bucciarelli-Rodriguez, E. Chartone-Souza, J.N. Silveira, A.P.S. Fontes, E.C. Pereira-Maia, J. Braz. Chem. Soc. 17 (2006) 1627.
[7] A. Garoufis, S.K. Hadjikakou, N. Hadjiliadis, Coord. Chem. Rev. 253 (2009) 1384.
[8] F.C.S. Paula, W. Guerra, I.R. Silva, J.N. Silveira, F.V. Botelho, L.Q. Vieira, E.C. Pereira-Maia, Chem. Biodiversity 5 (2008) 2124.
[9] W. Guerra, E.A. Azevedo, A.R.S. Monteiro, M. Bucciarelli-Rodriguez, E. Chartone-Souza, A.M.A. Nascimento, A.P.S. Fontes, L. Le Moyec, E.C. Pereira-Maia, J. Inorg. Biochem. 99 (2005) 2348.
[10] J.F. da Silva, W. Martins, Talanta 39 (1992) 1307.
[11] H. Okamura, N. Hirayama, K. Morita, K. Shimojo, H. Naganawa, H. Imura, Anal. Sci. 26 (2010) 607.
[12] M. Melchart, A. Habtemariam, S. Parsons, P.J. Sadler, J. Inorg. Biochem. 101 (2007) 1903;
S.A. De Pascali, A. Muscella, C. Vetrugno, S. Marsigliante, F.P. Fanizzi, Inorg. Chim. Acta 412 (2014) 88.
[13] J.J. Wilson, S.J. Lippard, J. Med. Chem. 55 (2012) 5326.
[14] D.F. Xu, Z.H. Shen, Y. Shi, Q. He, Q.C. Xia, Russian J. Coord. Chem. 36 (2010) 458.
[15] P.S. Lopes, D.A. Paixão, F.C.S. de Paula, A.M.D.C. Ferreira, J. Ellena, S. Guilardi, E.C. Pereira-Maia, W. Guerra, J. Mol. Struct. 1034 (2013) 84.
[16] J.H. Price, A.N. Williamson, R.F. Schramm, B.B. Wayland, Inorg. Chem. 11 (1972) 1280.
[17] S. Okeya, S.I. Ooi, K. Matsumoto, Y. Nakamura, S. Kawaguchi, Bull. Chem. Soc. Jpn. 54 (1981) 1085.
[18] M.W. Schmidt, K.K. Baldridge, J.A. Boatz, S.T. Elbert, M.S. Gordon, J.H. Jensen, S. Koseki, N. Matsunaga, K.A. Nguyen, S.J. Su, T.L. Windus, M. Dupuis, J.A. Montgomery, J. Comput. Chem. 14 (1993) 1347–1363.
[19] P.J. Hay, W.R. Wadt, J. Chem. Phys. 82 (1985) 299–310.
[20] (a) R. Ditchfie, W.J. Hehre, J.A. Pople, J. Chem. Phys. 54 (1971) 724;
(b) W.J. Hehre, R. Ditchfie, J.A. Pople, J. Chem. Phys. 56 (1972) 2257;
(c) M.M. Francl, W.J. Pietro, W.J. Hehre, J.S. Binkley, M.S. Gordon, D.J. Defrees, J.A. Pople, J. Chem. Phys. 77 (1982) 3654–3665;
(d) P. Harihara, J.A. Pople, Theor. Chim. Acta 28 (1973) 213–222.
[21] C. Adamo, V. Barone, J. Chem. Phys. 110 (1999) 6158–6169.
[22] (a) J.A. Bonacin, A.L.B. Formiga, V.H.S. de Melo, H.E. Toma, Vib. Spectrosc. 44 (2007) 133–141;
(b) R.A. Timm, J.A. Bonacin, A.L.B. Formiga, H.E. Toma, J. Braz. Chem. Soc. 19 (2008) 287–292.
[23] JMOL: an open-source Java viewer for chemical structures in 3D. <http://www.jmol.org>.
[24] J.C. Palomino, A. Martin, M. Camacho, H. Guerra, J. Swings, F. Portaela, Antimicrob. Agents Chemother. 46 (2002) 2720–2722.
[25] W. Geary, J. Coord. Chem. Rev. 7 (1971) 81.
[26] K. Nakamoto, Infrared, Raman Spectra of Inorganic and Coordination Compounds, fifth ed., Wiley, New York, 1997.
[27] Z. Chen, Y. Wu, F. Huang, D. Gu, F. Gan, Spectrochim. Acta 66 (2007) 1024.
[28] F.K. Keter, S. Kanyanda, S.L. Lyantagaye, J. Darkwa, D.J.P. Rees, M. Meyer, Cancer Chemother. Pharmacol. 63 (2008) 127.
[29] (a) M.A. Carvalho, R.E.F. de Paiva, F.R.G. Bergamini, A.F. Gomes, F.C. Gozzo, W.R. Lustri, A.L.B. Formiga, S.M. Shishido, C.V. Ferreira, P.P. Corbi, J. Mol. Struct. 1031 (2013) 125–131;
(b) R.E.F. de Paiva, C. Abbehausen, A.F. Gomes, F.C. Gozzo, W.R. Lustri, A.L.B. Formiga, P.P. Corbi, Polyhedron 36 (2012) 112–119.
[30] B. Lippert, Cisplatin Chemistry and Biochemistry of Leading Anticancer Drugs, first ed., Wiley-VCH, Germany, 1999.
[31] G.D. Souza, L.E. Fernandes, M.A. Rodrigues, P.P. Silva, E.C. Pereira-Maia, W. Guerra, Lat. Am. J. Pharm. 31 (2012) 620.
[32] G.D. de Souza, M.A.L.E. Fernandes, P.P. Silva, R. Ruggiero, E.C. Pereira-Maia, W. Guerra, Cent. Eur. J. Chem. 11 (2013) 290.
[33] P. Doležel, V. Kubáň, Chem. Pap. 56 (2002) 236.
[34] S.A. De Pascali, F. Lugoli, A. De Donno, F.P. Fanizzi, Met.-Based Drugs 2011 (2011) 763436.
[35] M. Mondelli, F. Pavan, P.C. de Souza, C.Q. Leite, J. Ellena, O.R. Nascimento, G. Facchin, M.H. Torre, J. Mol. Struct. 1036 (2013) 180.